Journal of Zhejiang University-SCIENCE B (Biomedicine & Biotechnology) 2021 22(11):929-940
www.jzus.zju.edu.cn; www.springer.com/journal/11585
E-mail: jzus_b@zju.edu.cn

Research Article

https://doi.org/10.1631/jzus.B2000583

Check for updates

Effect of Palrnatine on lipopolysaccharide-induced acute lung injury by inhibiting activation of the Akt/NF-κB pathway

Xingchi KAN[1], Yingsheng CHEN[1], Bingxu HUANG[1], Shoupeng FU[1], Wenjin GUO[1], Xin RAN[1], Yu CAO[1], Dianwen XU[1], Ji CHENG[1], Zhanqing YANG[1], Yanling XU[2]✉

[1]*Department of Theoretic Veterinary Medicine, College of Veterinary Medicine, Jilin University, Changchun 130012, China*
[2]*Department of Respiratory Medicine, the Second Hospital, Jilin University, Changchun 130012, China*

Abstract: Inflammation plays an important role in the development of acute lung injury (ALI). Severe pulmonary inflammation can cause acute respiratory distress syndrome (ARDS) or even death. Expression of proinflammatory interleukin-1β (IL-1β) and inducible nitric oxide synthase (iNOS) in the process of pulmonary inflammation will further exacerbate the severity of ALI. The purpose of this study was to explore the effect of Palrnatine (Pa) on lipopolysaccharide (LPS)-induced mouse ALI and its underlying mechanism. Pa, a natural product, has a wide range of pharmacological activities with the potential to protect against lung injury. Western blotting and quantitative real-time polymerase chain reaction (qRT-PCR) assays were performed to detect the expression and translation of inflammatory genes and proteins in vitro and in vivo. Immunoprecipitation was used to detect the degree of P65 translocation into the nucleus. We also used molecular modeling to further clarify the mechanism of action. The results showed that Pa pretreatment could significantly inhibit the expression and secretion of the inflammatory cytokine IL-1β, and significantly reduce the protein level of the proinflammatory protease iNOS, in both in vivo and in vitro models induced by LPS. Further mechanism studies showed that Pa could significantly inhibit the activation of the protein kinase B (Akt)/nuclear factor-κB (NF-κB) signaling pathway in the LPS-induced ALI mode and in LPS-induced RAW264.7 cells. Through molecular dynamics simulation, we observed that Pa was bound to the catalytic pocket of Akt and effectively inhibited the biological activity of Akt. These results indicated that Pa significantly relieves LPS-induced ALI by activating the Akt/NF-κB signaling pathway.

Key words: Acute lung injury; Palrnatine; Lipopolysaccharide (LPS); Protein kinase B/nuclear factor-κB (Akt/NF-κB)

1 Introduction

Acute lung injury (ALI) is a serious acute respiratory disease (Ning et al., 2020; Song et al., 2020), and its main characteristics are rapid onset, high incidence, and a mortality rate of more than 45% (Briel et al., 2010). Progression of the disease will induce the occurrence of acute respiratory distress syndrome (ARDS), which will lead to severe respiratory obstruction and further increase the risk of mortality (Bellingan, 2002); therefore, ALI is a serious threat to human health. At present, the main treatment methods for ALI include the treatment of primary diseases, respiratory support treatment, sedation treatment, and circulatory function support. However, there is still a lack of effective specific drugs (Bellingan, 2002; The National Heart, Lung, and Blood Institute Acute Respiratory Distress Syndrome (ARDS) Clinical Trials Network, 2006). Therefore, the search for a specific drug with significant effect and few side effects, which is conducive to improved prognosis, is very urgent.

The uncontrolled inflammatory response of lung tissue is the main cause of ALI and the usual source of inflammation is infection by Gram-negative bacteria (Goodman et al., 2003). Lipopolysaccharide (LPS) is the main virulence factor on the cell wall surface of Gram-negative bacteria. It is a common pathogenic factor in intensive care unit (ICU) wards, operating rooms, and other environments. It can induce the production of proinflammatory mediators and aggravate the severity of inflammatory reactions (Zilberberg and Epstein, 1998). Therefore, many studies have shown

✉ Yanling XU, xuyanling0719@sina.com
Yanling XU, https://orcid.org/0000-0002-0544-6517
Xingchi KAN, https://orcid.org/0000-0002-3541-4997

Received Sept. 23, 2020; Revision accepted Feb. 21, 2021;
Crosschecked Oct. 14, 2021

that the deterioration of ALI or ARDS disease can be alleviated by inhibiting the release of proinflammatory mediators and effectively controlling the inflammatory response (Yi et al., 2019; Patel et al., 2020). Nasal injection of LPS can effectively simulate pathogenesis of ALI, and is widely used in in vivo mice model (Mei et al., 2007). Alveolar macrophages are important immune cells in lung tissue, and RAW264.7 cell is a macrophage cell line (He et al., 2016). The LPS-induced RAW264.7 cell model is a commonly used in vitro model (Hou et al., 2018). Scientists often use the two LPS-induced in vivo and in vitro models as a basis for screening clinical drug candidates.

Nuclear factor-κB (NF-κB) signaling is closely related to the severity of ALI and ARDS diseases (Hou et al., 2018). As an important transcription factor, activation of NF-κB can promote expression of inflammatory mediators such as inflammatory cytokines (tumor necrosis factor-α (TNF-α), interleukin-1β (IL-1β), and IL-6) (Nennig and Schank, 2017; Kan et al., 2019; Xiang et al., 2019) and the proinflammatory proteases (inducible nitric oxide synthase (iNOS) and cyclooxygenase-2 (COX-2)) (Gao et al., 2017). A strong inflammatory response is one of the main symptoms of ALI. Studies have shown that phosphorylation of NF-κB can aggravate the severity of ALI (Buccelletti et al., 2003; Pedrazza et al., 2017). In addition, activation of the NF-κB signaling pathway is often closely related to inflammatory diseases, such as ALI (Tang et al., 2021), inflammatory bowel disease (Sangaraju et al., 2019), mastitis (Kan et al., 2019), and pneumonia (Hou et al., 2018). Therefore, inhibiting the phosphorylation of NF-κB is a potential therapeutic target to effectively alleviate the symptoms of ALI and ARDS (Pedrazza et al., 2017). Our previous results showed that the effective inhibition of NF-κB activation could significantly alleviate the symptoms of mastitis (Guo et al., 2019) and neuroinflammation (Fu et al., 2015). Furthermore, Hou et al. (2018) have shown that effective inhibition of NF-κB activation alleviates the symptoms of pneumonia. Therefore, effective inhibition of NF-κB activation in lung tissue is a potential treatment approach for ALI, and thus a very meaningful research direction.

Palrnatine (Pa), a natural product extracted from the plant *Fibraurea recisa* Pierre, has a wide range of biological activities, such as resisting bacterial infection and relieving inflammatory reaction (Yan et al., 2017; Mai et al., 2019). Mai et al. (2019) have shown that Pa inhibits inflammatory bowel disease by effectively inhibiting the inflammatory response. However, it has not been reported whether Pa has a therapeutic effect on ALI. Therefore, the purpose of this study was to investigate the effect of Pa on ALI and its potential mechanism in LPS-induced in vivo and in vitro models.

2 Materials and methods

2.1 Materials

Pa (≥98%, high-performance liquid chromatography (HPLC)) was purchased from Shanghai Yuanye Bio-Technology Co., Ltd. (Shanghai, China). Bovine serum albumin (BSA), TRIzol, LPS, and *N*,*N*,*N*',*N*'-tetramethylethylenediamine (TEMED) were purchased from Sigma-Aldrich (Saint Louis, MO, USA). The Primers were purchased from Shengong Biological Engineering Co., Ltd. (Shanghai, China). PrimeScript™ reverse transcription (RT) reagent kits (https://www.takarabiomed.com.cn/DownLoad/RR037A.pdf) and 2× SYBR Premix were purchased from TaKaRa Biomedical Technology Co., Ltd. (Kyoto, Japan). An enzyme-linked immunosorbent assay (ELISA) kit was purchased from Beijing Solarbio Science & Technology Co., Ltd. (Solarbio Science, Beijing, China). Dulbecco's modified Eagle's medium (DMEM), 4-(2-hydroxyethyl)-1-piperazineethanesulfonic acid (HEPES), and 25 g/mL trypsin were purchased from Thermo Fisher Scientific Inc. (Gibco, NY, USA). Primary antibodies (protein kinase B (Akt), phosphorylated Akt (p-Akt), P65, p-P65, inhibitor of NF-κB (IκB), p-IκB, and β-actin) were purchased from Cell Signaling Technology, Inc. (Danvers, MA, USA). Secondary antibodies (goat anti-mice and goat anti-rabbit) were provided by Boster Biological Technology Co., Ltd. (Hubei, China). Non-fat dry milk was purchased from Watson Technology Co., Ltd. (Beijing, China). A bicinchoninic acid (BCA) protein assay kit and radio immunoprecipitation assay (RIPA) lysate (P0013) were purchased from Shanghai Biyuntian Biotechnology Co., Ltd. (Shanghai, China). Fetal bovine serum (FBS) was purchased from Clark Bioscience (VA, USA). Tropifluor polyvinylidene fluoride (PVDF) transfer membrane was purchased from Thermo Fisher Technology Co., Ltd. (Shanghai, China). Super ECL Plus (P1050) was

purchased from Applygen Technologies, Inc. (Beijing, China).

2.2 Animals

Forty male Institute of Cancer Research (ICR) mice aged 6–8 weeks (Changsheng Biotechnology, Shenyang, China) were divided into four groups, each containing ten mice: no treatment group (NT), ALI model group (LPS), Pa group alone (Pa), and Pa treatment group (LPS+Pa). The mice ate and drank freely, and were given 12 h of light and dark cycles.

2.3 ALI model

The mice were held in one hand in a supine position. A total of 50 μg LPS was dissolved in 20 μL phosphate-buffered saline (PBS) solution and then infused into one side of each mouse's nasal cavity through a micro syringe. LPS was injected between breaths and injection was continued at a slow rate. When LPS injection was completed, the mice were gently rotated to evenly distribute LPS in the lungs.

2.4 Administration of Pa

Pa was administered by oral gavage with a concentration of 100 mg/kg and a volume of 100 μL for 6 d, and 100 μmol/L Pa was added to DMEM without FBS to stimulate RAW264.7 cells for 1 h. Pa was dissolved in normal saline solution and then stored at −20 ℃.

2.5 Cell culture

RAW264.7 cells were cultured in 37 ℃ constant-temperature incubators. When the fusion degree of cells reached 70%, 25 g/mL trypsin was used to digest cells for 3 min. The cells were evenly inoculated in a 60-cm^2 culture dish and 2 mL DMEM medium was added. When cell density reached 70%, 100 μmol/L Pa was added to stimulate the cells for 1 h, and then 1 μL of 1 μg/μL LPS was added to stimulate the cells for 4 h. Finally, cell samples were collected.

2.6 Histopathological examination

Fresh lung tissue blocks were soaked in formaldehyde for 48 h and then placed in 75% (volume fraction) alcohol. The paraffin section was produced by dehydration, embedding, sectioning, staining, and sealing. Finally, we observed the pathological damage to the lung tissue under a microscope and scored the tissue damage. The scoring content included indicators of alveolar integrity, pulmonary edema, pulmonary hemorrhage, and alveolar interstitial thickness. We assigned a score of 0 for no damage, 1 for mild damage, 2 for moderate damage, 3 for severe damage, and 4 for extreme damage (Lv et al., 2017).

2.7 ELISA assay

ICR mice were injected with 100 μL of sodium pentobarbital, and after the mice were anesthetized, the abdominal aorta was cut to release the blood in the blood vessels, in order to reduce lung congestion. Immediately, the mouse trachea was perfused with 1 mL of PBS into the lungs and washed twice, and finally about 600 μL of alveolar lavage fluid was aspirated for subsequent experiments.

We added 1 μL of IL-1β primary antibody to 200 μL of the sample dilution solution, and then added the diluted primary antibody to the bottom of the 96-well plate (100 μL per well), which was placed in a 4 ℃ refrigerator overnight. The next day, the supernatant was removed from the 96-well plate and rinsed four times with washing solution for 5 min each well. We then blocked the 96-well plate with 0.05 g/mL BSA for 2 h, incubated the secondary antibody for 1 h, catalyzed with horseradish peroxidase (HRP) for 30 min, and added 100 μL of 2 mol/L concentrated sulfuric acid to each well to stop the reaction. Note that after each step was completed, we used washing solution to rinse the plate four times, and finally measured the absorbance with a microplate reader (Bio-Rad, iMark, Shanghai, China).

2.8 Real-time PCR assay

The primers were designed on the National Center for Biotechnology Information (NCBI) website (https://www.ncbi.nlm.nih.gov/gene) in advance and then synthesized and stored in a −20 ℃ refrigerator for future use. TRIzol was added to RAW264.7 cells to extract total RNA. The experiment was performed according to the two-step reverse transcription instructions of the TaKaRa PrimeScript™ RT reagent kit. The reaction volume of quantitative real-time polymerase chain reaction (qRT-PCR) was 20 μL, including 1 μL of upstream primer, 1 μL of downstream primer, 8 μL of total complementary DNA (cDNA) , and 10 μL of SYBR Premix. The reaction conditions were 95 ℃ for 4 min, 95 ℃ for 40 s, and 60 ℃ for 30 s. A total

of 40 cycles were performed. Finally, the data were analyzed using Bio-Rad CFX Manager software (Bio-Rad, Shanghai, China).

The sequences of primers used in this experiment were as follows: IL-1β, forward 5'-GCTGCTTCCAAACCTTTGAC-3', reverse 5'-AGCTTCTCCACAGCCACAAT-3'; β-actin, forward 5'-ATCACTATTGGCAACGAGCGGTTC-3', reverse 5'-CAGCACTGTGTTGGCATAGAGGTC-3'.

2.9 Western blot

We added 400 μL of protein lysate to 0.1 g of lung tissue, which was ground in a tissue grinder for 10 min. We then added protein lysate to RAW264.7 cells to lyse for 30 min. Protein concentration was determined according to the BCA protein assay kit protocol. Based on the number of samples, we prepared an appropriate amount of BCA working solution: 50 mL of BCA reagent A plus 1 mL of BCA reagent B (50:1). The time for the reaction between the BCA working solution and protein sample was 20 min. The protein sample was added to a 12% sodiumdodecyl sulfate-polyacrylamide gel electrophoresis (SDS-PAGE), and the electrophoresis was performed at 110 V for 70 min; then the PVDF membrane was transferred at 100 V for 90 min. The PVDF membrane containing total protein was then sealed with 0.05 g/mL milk. We added 1 μL of primary antibody into 1000 μL of solution containing 0.05 g/mL BSA and mixed evenly, then brought the diluted primary antibody into contact with the PVDF membrane, and shook it overnight at 50 r/min in a 4 °C refrigerator. On the next day, the PVDF membrane was rinsed with 1× TBST (Tris-base 10 mmol/L, NaCl 150 mmol/L, and Tween-20 0.05% (volume fraction); Beijing Solarbio Science & Technology Co., Ltd., China) four times with 10 min each time. We added 1 μL of secondary antibody into 5000 μL of 0.05 g/mL milk, and then put the PVDF membrane into the second antibody solution. ECL ultrasensitive luminescent liquids A and B were mixed thoroughly in equal volumes and then added dropwise onto the PVDF membrane to obtain protein expression information on the PVDF membrane.

2.10 Immunofluorescence assay

To detect the inhibitory effect of Pa on the NF-κB signaling pathway, we measured the translocation of P65 into the nucleus. RAW264.7 cells were evenly seeded in 24-well plates prepared with sterile glass climbing sheet. The cell density was kept low to prevent contact between cells from affecting morphological observations. After 12 h, the medium was removed, and the cells were fixed with 0.04 g/mL formaldehyde solution and sealed with 0.05 g/mL goat serum for 1 h. The first antibody (1:100 (volume ratio) in 0.05 g/mL BSA) was then added into the cell slides, which were put into 4 °C refrigerators overnight. The second fluorescent antibody (1: 100 (volume ratio) in 0.05 g/mL BSA) was added the next day to keep it away from light. In the next step, 40 μL 2-(4-amidinophenyl)-6-indolecarbamidine dihydrochloride (DAPI) was added to each climbing piece to label the nucleus. Finally, we obtained the experimental results by immunofluorescence.

2.11 Molecular dynamics simulation

The three-dimensional (3D) model of Akt was obtained from the Protein Data Bank (PDB, https://www.rcsb.org), and the 3D model of Pa was obtained from the ChemSpider website (https://www.chemspider.com). AutoDock 4 (http://autodock.scripps.edu) was used to simulate the molecular dynamics process of a complex Akt-PA system by docking protein with Pa. The details of the computational biology method were taken from the experimental methods (Liu et al., 2019).

2.12 Statistical analysis

Graphpad Prism 8.0 (https://www.graphpad.com/scientific-software/prism; Changchun, China) was used to analyze statistical data and create a histogram. The relative density of protein bands was analyzed with ImageJ software. The data were expressed as mean± standard error of mean (SEM). We used Dunnett's tests and one-way analysis of variance (ANOVA) to analyze differences between data. Student's *t*-test was used to compare two sets of data.

3 Results

3.1 Effects of Pa on lung histopathology in LPS-induced ALI

Pathological sections of lung tissues of mice were observed under a microscope with the following results. There was no histopathological damage in lung tissues of the NT or Pa alone groups, indicating that 100 mg/kg Pa orally had no toxic effect on the

mice (Figs. 1a, 1b, 1e, 1f, 1i, 1j, and 1k). However, in the LPS group, alveolar atrophy, alveolar interstitial thickness, and inflammatory cell infiltration increased. These results indicated that the ALI model was successfully constructed and that lung tissue was severely damaged during the ALI process (Figs. 1c, 1g, 1i, and 1k). It is interesting that Pa pretreatment can significantly alleviate the damage to the above pathological tissues (Figs. 1d, 1h, and 1i). These results preliminarily proved that Pa has a therapeutic effect on ALI.

3.2 Effects of Pa on IL-1β and iNOS in LPS-induced in vitro and in vivo models

IL-1β is an important inflammatory cytokine and iNOS is an important proinflammatory protease. These proinflammatory mediators can aggravate the inflammatory response. Therefore, we tracked changes of IL-1β and iNOS in vivo and in vitro. Compared with the NT group, Pa did not increase synthesis of IL-1β (Fig. 2d) or iNOS protein expression level (Figs. 2e and 2f) in lung tissue, further confirming that the selected Pa concentration was nontoxic; in vitro experimental results further verified this finding (Figs. 2a–2c). Compared with the NT group, LPS significantly increased the synthesis and expression of iNOS (Figs. 2b and 2c) as well as the mRNA level of *IL-1β* (Fig. 2a), which indicated that the inflammatory reaction was intense during the ALI process, and exacerbated the process of ALI. However, it is interesting to note that after Pa pretreatment, these inflammatory mediators were significantly inhibited, and this result was fully confirmed in both in vivo and in vitro experiments. These results further indicated that Pa had a significant therapeutic effect on ALI.

3.3 Effects of Pa on Akt/NF-κB in LPS-induced mice ALI

Akt/NF-κB is a classic inflammatory signaling pathway. Activation of this pathway can promote

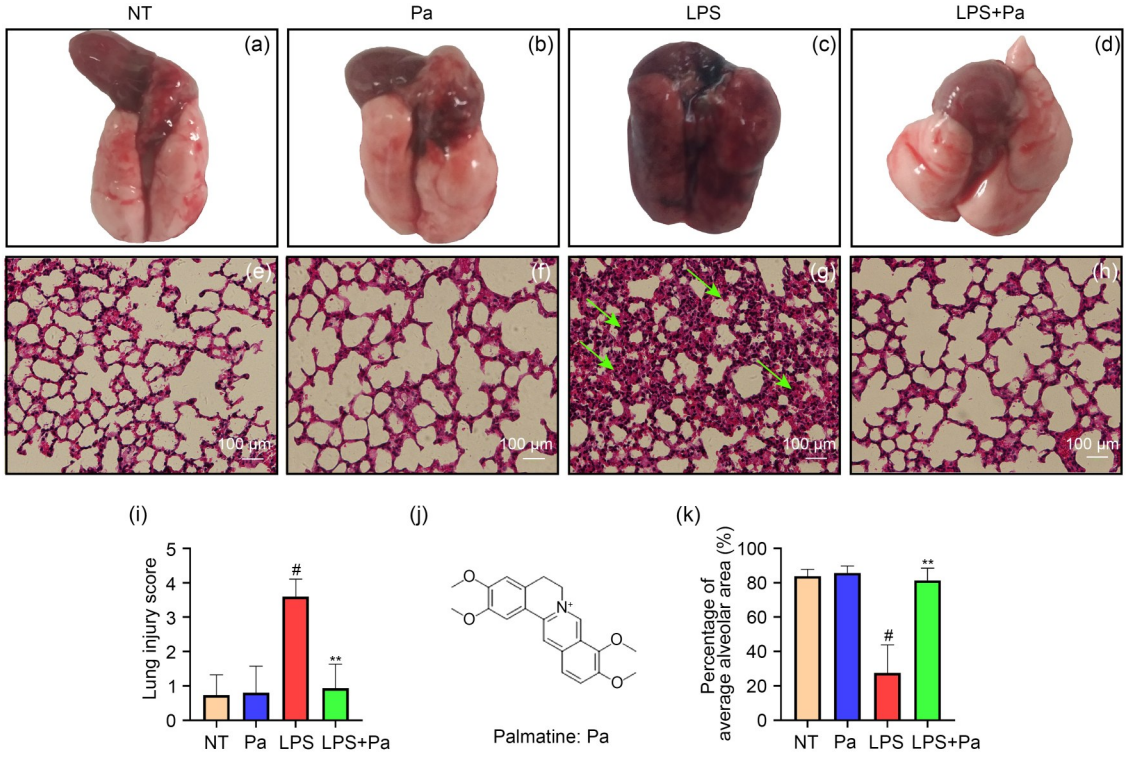

Fig. 1 Effect of Palrnatine (Pa) on lung histopathology in a lipopolysaccharide (LPS)-induced mice acute lung injury (ALI) model. (a–d) Photos of lungs from the no treatment (NT), Pa, LPS, and LPS+Pa groups; (e–h) Hematoxylin-eosin (HE)-stained sections of lungs from the NT, Pa, LPS, and LPS+Pa groups (scan bar=100 μm), in which arrows represent thickening of the stroma between the alveolar cavities; (i) Lung histopathological damage score; (j) Chemical structural formula of Pa; (k) Alveolar area as a percentage of total area. The data are expressed as mean±standard error of mean (SEM), n=10. $^{\#}$ P<0.01, vs. NT; ** P<0.01, vs. LPS.

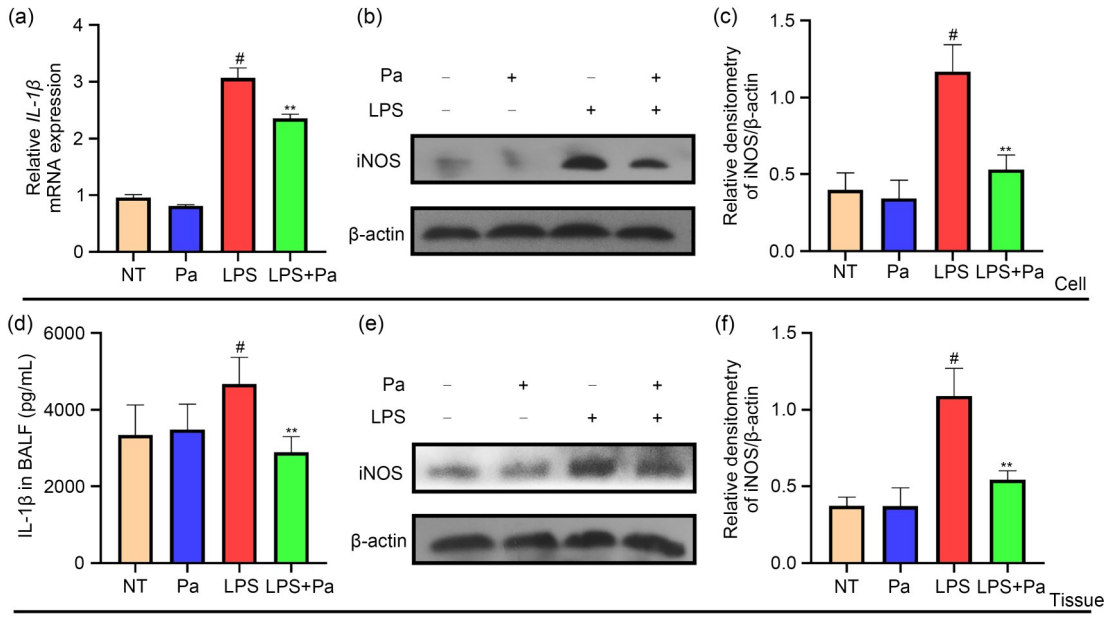

Fig. 2 Effects of Palrnatine (Pa) on interleukin-1β (IL-1β) and inducible nitric oxide synthase (iNOS) in lipopolysaccharide (LPS)-induced in vitro and in vivo models. (a–c) Expression of *IL-1β* mRNA (a), relative contents of proinflammatory protease iNOS and internal reference protein β-actin (b), and relative density of iNOS (c) in RAW264.7; (d–f) Concentration of IL-1β in bronchoalveolar lavage fluid (BALF) (d), relative contents of proinflammatory protease iNOS and internal reference protein β-actin (e), and relative density of iNOS (f) in lung tissues. Data are expressed as mean±standard error of mean (SEM), *n*=10. # *P*<0.01, vs. no treatment (NT); ** *P*<0.01, vs. LPS.

the expression of inflammatory factors, thereby exacerbating the severity of ALI. To elucidate the anti-inflammatory mechanism of Pa, we examined the changes to the Akt/NF-κB signaling pathway in lung tissue of ALI mice by western blot technology. LPS significantly activated Akt, p-P65, IκB, and protein phosphorylation levels, but Pa pretreatment significantly inhibited the phosphorylation levels of these proteins (Figs. 3a–3f). This showed that Pa played a role in the treatment of ALI by inhibiting activation of the Akt/NF-κB signaling pathway.

3.4 Effects of Pa on Akt/NF-κB in LPS-induced RAW264.7 cells

To further confirm the potential mechanism of Pa treatment for ALI, we tracked changes in the Akt/NF-κB signaling pathway in LPS-induced RAW264.7 cells by western blot. As expected, LPS significantly activated Akt, p-P65, IκB, and protein phosphorylation levels, but Pa pretreatment significantly inhibited the phosphorylation levels of these proteins (Figs. 4a–4f).

In addition, our results showed that LPS significantly promoted translocation of P65 into the nucleus. However, it is interesting that Pa pretreatment significantly inhibited this process (Figs. 5a–5b).

These results further confirmed that Pa has a therapeutic effect on ALI, and its mechanism is to inhibit the phosphorylation level of the Akt/NF-κB signaling pathway.

3.5 Molecular dynamics simulation for Akt

To explore the specific mechanism of Pa inhibiting Akt protein, we used AutoDock 4 software to predict and simulate the binding of Pa and Akt protein. The combination diagram of Akt and Pa is shown in Fig. 6. Hydrogen bonding was clearly observed for the binding of Pa to Akt. During the simulation, Pa was localized to the catalytic pocket of Akt THR-51. Specifically, the side chain of Akt, THR-51, had strong interaction with Pa. To explore the energy contributions from the residues of the binding sites in the Akt-Pa complex, we calculated the binding free energy decomposition. As shown in Fig. 6, the total binding energy was −6.59 kcal/mol, which has practical biological significance.

Our data suggested that Pa inhibited the biological activity of Akt by binding to the active region (THR-51 residue) of Akt, and thus inhibited the activation of inflammatory signaling pathways and the release of inflammatory mediators.

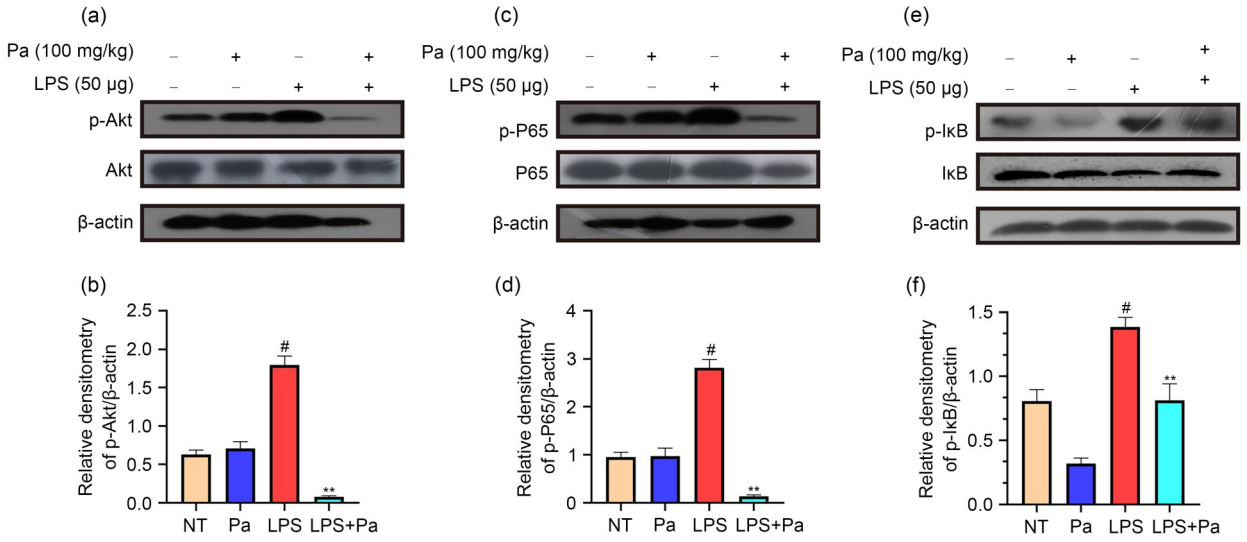

Fig. 3 Effects of Palrnatine (Pa) on protein kinase B (Akt)/nuclear factor-κB (NF-κB) in lipopolysaccharide (LPS)-induced mouse acute lung injury (ALI). Total protein of lung tissue was extracted 12 h after the ALI model was constructed. (a) Protein bands of Akt, phosphorylated Akt (p-Akt), and β-actin in lungs; (b) Relative density of protein band p-Akt; (c) Protein bands of P65, p-P65, and β-actin in lungs; (d) Relative density of protein band p-P65; (e) Protein bands of inhibitor of NF-κB (IκB), p-IκB, and β-actin in lungs; (f) Relative density of protein band p-IκB. Data are expressed as mean±standard error of mean (SEM), *n*=10. $^{\#}$ *P*<0.01, vs. no treatment (NT); ** *P*<0.01, vs. LPS.

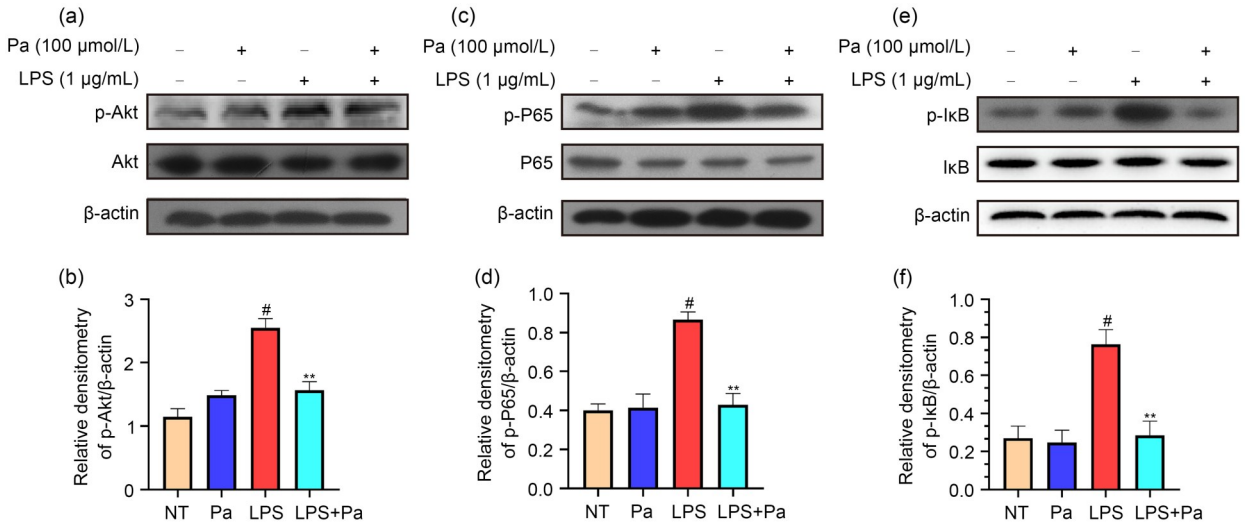

Fig. 4 Effects of Palrnatine (Pa) on protein kinase B (Akt)/nuclear factor-κB (NF-κB) in lipopolysaccharide (LPS)-induced RAW264.7 cells. Total protein of RAW264.7 was extracted 4 h after LPS stimulation. (a) Protein bands of Akt, phosphorylated Akt (p-Akt), and β-actin in cells; (b) Relative density of protein band p-Akt; (c) Protein bands of P65, p-P65, and β-actin in lungs; (d) Relative density of protein band p-P65; (e) Protein bands of inhibitor of NF-κB (IκB), p-IκB, and β-actin in cells; (f) Relative density of protein band p-IκB. Data are expressed as mean±standard error of mean (SEM), *n*=3. $^{\#}$ *P*<0.01, vs. no treatment (NT); ** *P*<0.01, vs. LPS.

4 Discussion

Inflammatory response is closely related to ALI, and it is now widely believed that strong inflammatory response is the main factor leading to ALI (Tsushima et al., 2009; Soni et al., 2016). When inflammatory secretions and inflammatory cytokines are produced during the inflammatory response, respiratory stress is increased and the structure of lung tissue is destroyed (Tsushima et al., 2009). Therefore, inhibiting

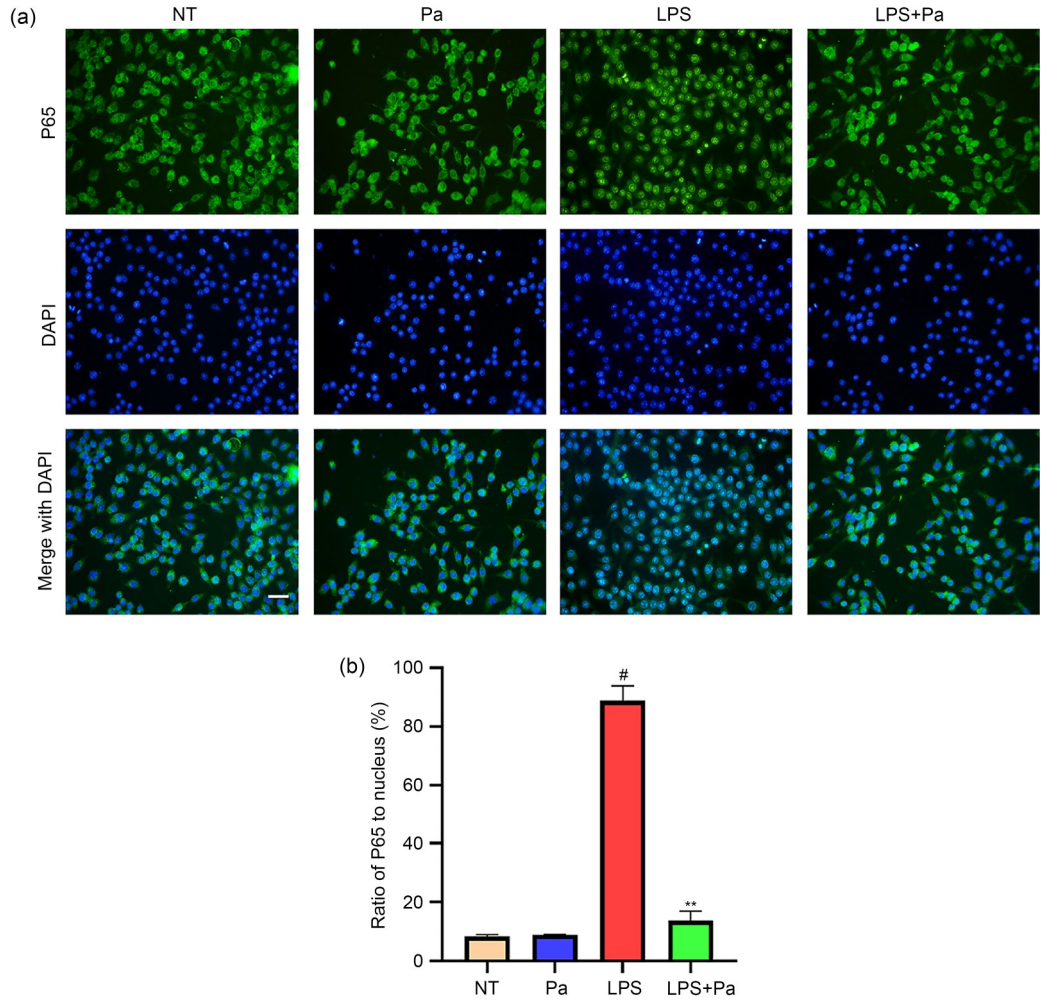

Fig. 5 Effects of Palrnatine (Pa) on P65 translocation into the nucleus in lipopolysaccharide (LPS)-induced RAW264.7 cells. Cells were pretreated with Pa for 1 h followed by LPS for 12 h. Fluorescence microscopy was used to assess translocation of P65 into the nucleus. (a) Immunofluorescence results of nuclear factor-κB (NF-κB) P65 entering the nucleus (scale bar= 100 μm); (b) Ratio of NF-κB P65 to nucleus. Data are expressed as mean±standard error of mean (SEM), *n*=3. # *P*<0.01, vs. no treatment (NT); ** *P*<0.01, vs. LPS. DAPI: 2-(4-amidinophenyl)-6-indolecarbamidine dihydrochloride.

inflammation of lung tissue is a potential treatment for ALI. In this study, we found that Pa significantly inhibited the expression and secretion of the proinflammatory protease iNOS and the inflammatory cytokine IL-1β in both LPS-induced in vivo and in vitro models, and further studied its mechanism.

Inflammation plays an important role in the development of disease (Zhang et al., 2019; Deng et al., 2020; Song et al., 2020; Ye et al., 2020; Zhao et al., 2020), and the inflammatory response causes macrophages to synthesize a large number of proinflammatory mediators, such as iNOS and nitric oxide (NO) (Hou et al., 2018). Excessive production of iNOS and NO is closely related to the occurrence and development of many lung diseases, such as pneumonia and even ARDS (Song et al., 2018); therefore, any substance that inhibits iNOS may alleviate the occurrence of lung diseases. In addition, the overactivation of macrophages can also produce IL-1β, TNF-α, IL-6, and other inflammatory cytokines (Hou et al., 2018), among which IL-1β is the most representative inflammatory mediator (Zheng et al., 2018). Normal inflammatory response is beneficial to the body, but when stimulated by strong pathogenic factors such as endotoxins, macrophages are overactivated to produce too many inflammatory cytokines (Zeytun et al., 2010), which aggravate the inflammatory reaction process and lead to ALI (Gandhirajan et al., 2013). Therefore, any substance that inhibits the production of inflammatory cytokines such as IL-1β is a potential therapeutic drug

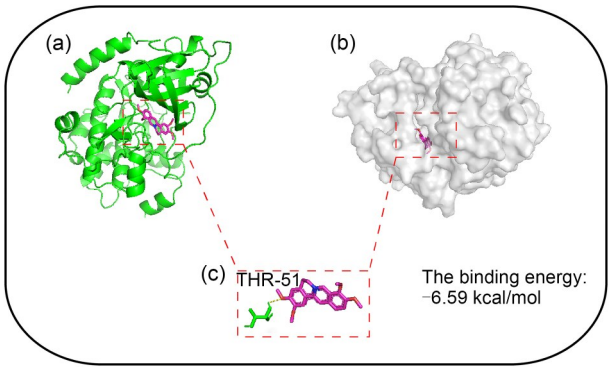

Fig. 6 Three-dimensional (3D) structures of protein kinase B (Akt) with Palrnatine (Pa). (a) Cartoon model of Akt and Pa complex; (b) Surface model of Akt and Pa complex; (c) Binding of amino acid residue THR-51 of AKT with Pa. Pink represents Pa. The total energy is −6.59 kcal/mol (Note: for interpretation of the references to color in this figure legend, the reader is referred to the web version of this article).

for the treatment of ALI. The results showed that Pa could significantly inhibit the LPS-induced expression and secretion of iNOS and IL-1β in vitro and in vivo. Thus, it appears that Pa plays a role in the treatment of ALI by inhibiting the production of inflammatory mediators.

To elucidate the mechanism by which Pa inhibits the production of LPS-induced proinflammatory protease and proinflammatory factors, we examined the effects of Pa on Akt signaling in LPS-induced in vitro and in vivo models, further explored the interaction mechanism between Pa and Akt, and carried out molecular dynamics simulation on the Akt-Pa complex system. Studies have shown that LPS binds to Toll-like receptor 4 (TLR4) and transmits inflammation signals to the downstream protein kinase Akt (Slomiany and Slomiany, 2017; Jeon et al., 2020). Akt protein is significantly increased at the onset of inflammation (Goodman et al., 2003; Jin et al., 2020), and p-Akt can induce increased expression of inflammatory cytokines IL-1β, TNF-α, and IL-6 and inflammatory protease iNOS (Guo et al., 2019; Kan et al., 2019). A large number of proinflammatory mediators stimulate a strong immune response, which exacerbates the occurrence and development of ALI (Goodman et al., 2003). It has been reported that myrnicetin can alleviate the severity of pneumonia by inhibiting the activation of Akt protein (Hou et al., 2018). Therefore, Akt may also be a therapeutic target for treating ALI disease. Our experimental results showed that Pa can significantly inhibit the activation of Akt in lung tissue in vivo, and this was further verified in the in vitro model. More importantly, we found that Pa could localize to the catalytic pocket of Akt, which is very close to the binding site of the substrate. Because of the binding of Pa with Akt, the binding of substrate with Akt was blocked, resulting in the loss of biological activity of Akt and preventing activation of downstream inflammatory signaling pathways by Akt, which effectively prevented the release of inflammatory mediators from aggravating ALI. Thus, the therapeutic effect of Pa on ALI is achieved by inhibiting the phosphorylation of Akt protein. In addition, a study by Yu et al. (2017) has pointed out that after activation of Akt, it further transmits inflammatory signals down to NF-κB.

NF-κB is an important inflammatory signaling pathway located in the downstream signaling pathway of Akt protein, whose action can aggravate inflammatory disease (Chauhan et al., 2018; Hou et al., 2018). Therefore, to further explore the inhibition of Pa on Akt, we explored the effect of Pa on the NF-κB signaling pathway in LPS-induced in vivo and in vitro models. Activation of NF-κB can promote the expression of the inflammatory cytokines IL-1β, TNF-α, and IL-6. In addition, the proinflammatory protease iNOS is also regulated by NF-κB signals (Yan et al., 2017; Hou et al., 2018). Under normal physiological conditions, P65 and IκB proteins are in a bound state, and NF-κB in this state has no proinflammatory activity (Fu et al., 2015). However, under the stimulation of other pathogenic factors such as LPS, IκB is phosphorylated and ubiquitinated, which promotes the translocation of NF-κB into the nucleus, prompts the release of inflammatory mediators, and exacerbates the response process of ALI (Metz and Sibbald, 1991). In addition, many studies rely on the level of NF-κB phosphorylation to reflect activation of the NF-κB pathway (Fu et al., 2015; Nennig and Schank, 2017), so we tracked the changes in NF-κB phosphorylation. We found that LPS can cause significant IκB phosphorylation and ubiquitination degradation, but Pa pretreatment can significantly inhibit IκB phosphorylation and ubiquitination degradation, which is beneficial to prevent the translocation of NF-κB into the nucleus. However, it is interesting to note that Pa pretreatment can significantly inhibit p-NF-κB P65 phosphate levels and the degree of P65 translocation into the nucleus. Thus, Pa inhibits the phosphorylation

level of Akt protein effectively and the activity of NF-κB, an inflammatory signaling pathway downstream of Akt. There are other potential mechanisms for the treatment of ALI by Pa, which still need further study.

5 Conclusions

Pa has a significant therapeutic effect on ALI, and its mechanism is to inhibit activation of the Akt/NF-κB signaling pathway (Fig. 7).

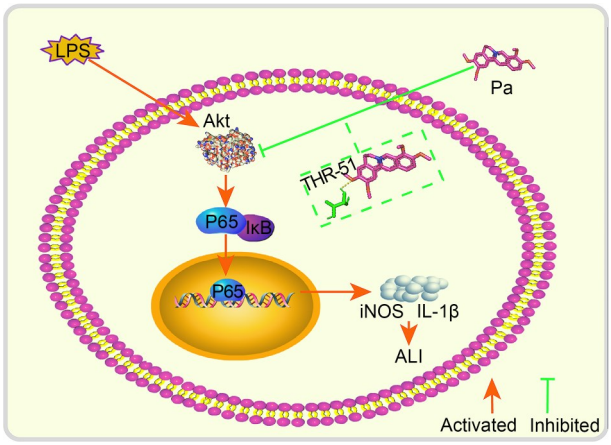

Fig. 7 Schematic summarizing the effect and mechanism of Palrnatine (Pa) on acute lung injury (ALI) in lipopolysaccharide (LPS)-induced RAW264.7 cells. LPS significantly activated protein kinase B (Akt)/nuclear factor-κB (NF-κB) signaling and promoted the release of inflammatory mediators in cells, which induced ALI. Pa administration significantly alleviated the LPS-induced inflammatory response of ALI by inhibiting Akt/NF-κB signaling. Furthermore, Pa may play a protective role by hydrogen bonding with the THR-51 of Akt protein. iNOS: inducible nitric oxide synthase; IL-1β: interleukin-1β.

Acknowledgments

This work was supported by the National Natural Science Foundation of China (Nos. 31672509 and 31873004), the Jilin Scientific and Technological Development Program (Nos. 20190103021JH and 20200201111JC), and the Jilin University (JLU) Science and Technology Innovative Research Team (No. 2017TD-30), China.

Author contributions

Xingchi KAN and Yanling XU designed and supervised the study. Xingchi KAN, Yingsheng CHEN, Bingxu HUANG, Wenjin GUO, Xin RAN, Yu CAO, Dianwen XU, Ji CHENG, and Zhanqing YANG performed the experiments. Xingchi KAN and Bingxu HUANG wrote the manuscript. Shoupeng FU revised the article. Shoupeng FU, Yu CAO, Dianwen XU, Ji CHENG, and Zhanqing YANG performed the statistical analyses. All authors have read and approved the final manuscript, and therefore, have full access to all the data in the study and take responsibility for the integrity and security of the data.

Compliance with ethics guidelines

Xingchi KAN, Yingsheng CHEN, Bingxu HUANG, Shoupeng FU, Wenjin GUO, Xin RAN, Yu CAO, Dianwen XU, Ji CHENG, Zhanqing YANG, and Yanling XU declare that they have no conflict of interest.

All institutional and national guidelines for the care and use of laboratory animals were followed. The study was approved by Animal Experiment Ethics Committee of Jilin University (No. SY202106010), China.

References

Bellingan GJ, 2002. The pulmonary physician in critical care · 6: the pathogenesis of ALI/ARDS. *Thorax*, 57(6):540-546. https://doi.org/10.1136/thorax.57.6.540

Briel M, Meade M, Mercat A, et al., 2010. Higher vs lower positive end-expiratory pressure in patients with acute lung injury and acute respiratory distress syndrome: systematic review and meta-analysis. *JAMA*, 303(9):865-873. https://doi.org/10.1001/jama.2010.218

Buccelletti F, Mazzone M, Portale G, et al., 2003. Humoral and cellular inflammatory mediators in acute lung injury: friends or enemies? *Minerva Med*, 94(3):157-165.

Chauhan PS, Singh DK, Dash D, et al., 2018. Intranasal curcumin regulates chronic asthma in mice by modulating NF-κB activation and MAPK signaling. *Phytomedicine*, 51:29-38. https://doi.org/10.1016/j.phymed.2018.06.022

Deng JW, Yang Q, Cai XP, et al., 2020. Early use of dexamethasone increases *Nr4a1* in Kupffer cells ameliorating acute liver failure in mice in a glucocorticoid receptor-dependent manner. *J Zhejiang Univ-Sci B (Biomed & Biotechnol)*, 21(9):727-739. https://doi.org/10.1631/jzus.B2000249

Fu SP, Wang JF, Xue WJ, et al., 2015. Anti-inflammatory effects of BHBA in both *in vivo* and *in vitro* Parkinson's disease models are mediated by GPR109A-dependent mechanisms. *J Neuroinflammation*, 12:9. https://doi.org/10.1186/s12974-014-0230-3

Gandhirajan RK, Meng S, Chandramoorthy HC, et al., 2013. Blockade of NOX2 and STIM1 signaling limits lipopolysaccharide-induced vascular inflammation. *J Clin Invest*, 123(2):887-902. https://doi.org/10.1172/JCI65647

Gao Y, Xiao XS, Zhang CL, et al., 2017. Melatonin synergizes the chemotherapeutic effect of 5-fluorouracil in colon cancer by suppressing PI3K/AKT and NF-κB/iNOS signaling pathways. *J Pineal Res*, 62(2):e12380. https://doi.org/10.1111/jpi.12380

Goodman RB, Pugin J, Lee JS, et al., 2003. Cytokine-mediated inflammation in acute lung injury. *Cytokine Growth Factor*

Rev, 14(6):523-535.
https://doi.org/10.1016/s1359-6101(03)00059-5

Guo WJ, Liu BR, Hu GQ, et al., 2019. Vanillin protects the blood-milk barrier and inhibits the inflammatory response in LPS-induced mastitis in mice. *Toxicol Appl Pharmacol*, 365:9-18.
https://doi.org/10.1016/j.taap.2018.12.022

He M, Ichinose T, Song Y, et al., 2016. Desert dust induces TLR signaling to trigger Th2-dominant lung allergic inflammation *via* a MyD88-dependent signaling pathway. *Toxicol Appl Pharmacol*, 296:61-72.
https://doi.org/10.1016/j.taap.2016.02.011

Hou W, Hu SY, Su ZZ, et al., 2018. Myricetin attenuates LPS-induced inflammation in RAW 264.7 macrophages and mouse models. *Future Med Chem*, 10(19):2253-2264.
https://doi.org/10.4155/fmc-2018-0172

Jeon J, Lee Y, Yu H, et al., 2020. HSP70-homolog DnaK of *Pseudomonas aeruginosa* increases the production of IL-27 through expression of *EBI3* via TLR4-dependent NF-κB and TLR4-independent Akt signaling. *Int J Mol Sci*, 21(23):9194.
https://doi.org/10.3390/ijms21239194

Jin MY, Feng HH, Wang Y, et al., 2020. Gentiopicroside ameliorates oxidative stress and lipid accumulation through nuclear factor erythroid 2-related factor 2 activation. *Oxid Med Cell Longev*, 2020:2940746.
https://doi.org/10.1155/2020/2940746

Kan XC, Liu BR, Guo WJ, et al., 2019. Myricetin relieves LPS-induced mastitis by inhibiting inflammatory response and repairing the blood-milk barrier. *J Cell Physiol*, 234(9):16252-16262.
https://doi.org/10.1002/jcp.28288

Liu S, Zhang J, Zhou YL, et al., 2019. Pterostilbene restores carbapenem susceptibility in New Delhi metallo-β-lactamase-producing isolates by inhibiting the activity of New Delhi metallo-β-lactamases. *Br J Pharmacol*, 176(23):4548-4557.
https://doi.org/10.1111/bph.14818

Lv HM, Liu QM, Wen ZM, et al., 2017. Xanthohumol ameliorates lipopolysaccharide (LPS)-induced acute lung injury via induction of AMPK/GSK3β-Nrf2 signal axis. *Redox Biol*, 12:311-324.
https://doi.org/10.1016/j.redox.2017.03.001

Mai CT, Wu MM, Wang CL, et al., 2019. Palmatine attenuated dextran sulfate sodium (DSS)-induced colitis via promoting mitophagy-mediated NLRP3 inflammasome inactivation. *Mol Immunol*, 105:76-85.
https://doi.org/10.1016/j.molimm.2018.10.015

Mei SH, McCarter SD, Deng YP, et al., 2007. Prevention of LPS-induced acute lung injury in mice by mesenchymal stem cells overexpressing angiopoietin 1. *PLoS Med*, 4(9): e269.
https://doi.org/10.1371/journal.pmed.0040269

Metz C, Sibbald WJ, 1991. Anti-inflammatory therapy for acute lung injury: a review of animal and clinical studies. *Chest J*, 100(4):1110-1119.
https://doi.org/10.1378/chest.100.4.1110

Nennig SE, Schank JR, 2017. The role of NFkB in drug addiction: beyond inflammation. *Alcohol Alcohol*, 52(2): 172-179.
https://doi.org/10.1093/alcalc/agw098

Ning K, Guan ZB, Lu HT, et al., 2020. Lung macrophages are involved in lung injury secondary to repetitive diving. *J Zhejiang Univ-Sci B (Biomed & Biotechnol)*, 21(8):646-656.
https://doi.org/10.1631/jzus.B1900687

Patel A, Khande H, Periasamy H, et al., 2020. Immunomodulatory effect of doxycycline ameliorates systemic and pulmonary inflammation in a murine polymicrobial sepsis model. *Inflammation*, 43(3):1035-1043.
https://doi.org/10.1007/s10753-020-01188-y

Pedrazza L, Cunha AA, Luft C, et al., 2017. Mesenchymal stem cells improves survival in LPS-induced acute lung injury acting through inhibition of NETs formation. *J Cell Physiol*, 232(12):3552-3564.
https://doi.org/10.1002/jcp.25816

Sangaraju R, Nalban N, Alavala S, et al., 2019. Protective effect of galangin against dextran sulfate sodium (DSS)-induced ulcerative colitis in Balb/c mice. *Inflamm Res*, 68(8):691-704.
https://doi.org/10.1007/s00011-019-01252-w

Slomiany BL, Slomiany A, 2017. Role of LPS-elicited signaling in triggering gastric mucosal inflammatory responses to *H. pylori*: modulatory effect of ghrelin. *Inflammopharmacology*, 25(4):415-429.
https://doi.org/10.1007/s10787-017-0360-1

Song CY, Xu YG, Lu YQ, 2020. Use of *Tripterygium wilfordii* Hook F for immune-mediated inflammatory diseases: progress and future prospects. *J Zhejiang Univ-Sci B (Biomed & Biotechnol)*, 21(4):280-290.
https://doi.org/10.1631/jzus.B1900607

Song YD, Wu YX, Li XZ, et al., 2018. Protostemonine attenuates alternatively activated macrophage and DRA-induced asthmatic inflammation. *Biochem Pharmacol*, 155:198-206.
https://doi.org/10.1016/j.bcp.2018.07.003

Soni S, Wilson MR, O'Dea KP, et al., 2016. Alveolar macrophage-derived microvesicles mediate acute lung injury. *Thorax*, 71(11):1020-1029.
https://doi.org/10.1136/thoraxjnl-2015-208032

Tang J, Xu LQ, Zeng YW, et al., 2021. Effect of gut microbiota on LPS-induced acute lung injury by regulating the TLR4/NF-κB signaling pathway. *Int Immunopharmacol*, 91:107272.
https://doi.org/10.1016/j.intimp.2020.107272

The National Heart, Lung, and Blood Institute Acute Respiratory Distress Syndrome (ARDS) Clinical Trials Network, 2006. Pulmonary-artery versus central venous catheter to guide treatment of acute lung injury. *N Engl J Med*, 354(21):2213-2224.
https://doi.org/10.1056/NEJMoa061895

Tsushima K, King LS, Aggarwal NR, et al., 2009. Acute lung injury review. *Intern Med*, 48(9):621-630.
https://doi.org/10.2169/internalmedicine.48.1741

Xiang YN, Guo ZM, Zhu PF, et al., 2019. Traditional Chinese medicine as a cancer treatment: modern perspectives of ancient but advanced science. *Cancer Med*, 8(5):1958-1975.

https://doi.org/10.1002/cam4.2108

Yan BQ, Wang DS, Dong SW, et al., 2017. Palmatine inhibits TRIF-dependent NF-κB pathway against inflammation induced by LPS in goat endometrial epithelial cells. *Int Immunopharmacol*, 45:194-200. https://doi.org/10.1016/j.intimp.2017.02.004

Ye ZH, Ning K, Ander BP, et al., 2020. Therapeutic effect of methane and its mechanism in disease treatment. *J Zhejiang Univ-Sci B (Biomed & Biotechnol)*, 21(8):593-602. https://doi.org/10.1631/jzus.B1900629

Yi L, Zhou ZD, Zheng YJ, et al., 2019. Suppressive effects of GSS on lipopolysaccharide-induced endothelial cell injury and ALI via TNF-α and IL-6. *Mediat Inflamm*, 2019: 4251394. https://doi.org/10.1155/2019/4251394

Yu ML, Qi BQ, Wu XX, et al., 2017. Baicalein increases cisplatin sensitivity of A549 lung adenocarcinoma cells via PI3K/Akt/NF-κB pathway. *Biomed Pharmacother*, 90:677-685. https://doi.org/10.1016/j.biopha.2017.04.001

Zeytun A, Chaudhary A, Pardington P, et al., 2010. Induction of cytokines and chemokines by Toll-like receptor signaling: strategies for control of infammation. *Crit Rev Immunol*, 30(1):53-67. https://doi.org/10.1615/critrevimmunol.v30.i1.40

Zhang H, Wu ZM, Yang YP, et al., 2019. Catalpol ameliorates LPS-induced endometritis by inhibiting inflammation and TLR4/NF-κB signaling. *J Zhejiang Univ-Sci B (Biomed & Biotechnol)*, 20(10):816-827. https://doi.org/10.1631/jzus.B1900071

Zhao K, Yang CX, Li P, et al., 2020. Epigenetic role of N^6-methyladenosine (m^6A) RNA methylation in the cardiovascular system. *J Zhejiang Univ-Sci B (Biomed & Biotechnol)*, 21(7):509-523. https://doi.org/10.1631/jzus.B1900680

Zheng WH, Chen CH, Zhang CX, et al., 2018. The protective effect of phloretin in osteoarthritis: an *in vitro* and *in vivo* study. *Food Funct*, 9(1):263-278. https://doi.org/10.1039/c7fo01199g

Zilberberg MD, Epstein SK, 1998. Acute lung injury in the medical ICU: comorbid conditions, age, etiology, and hospital outcome. *Am J Respir Crit Care Med*, 157(4 Pt 1): 1159-1164. https://doi.org/10.1164/ajrccm.157.4.9704088